Microfluid Nanofluid (2010) 8:709–726
DOI 10.1007/s10404-010-0588-1

REVIEW

Advances and applications on microfluidic velocimetry techniques

Stuart J. Williams · Choongbae Park · Steven T. Wereley

Received: 26 June 2009 / Accepted: 19 February 2010 / Published online: 24 March 2010
© Springer-Verlag 2010

Abstract The development and analysis of the performance of microfluidic components for lab-on-a-chip devices are becoming increasingly important because microfluidic applications are continuing to expand in the fields of biology, nanotechnology, and manufacturing. Therefore, the characterization of fluid behavior at the scales of micro- and nanometer levels is essential. A variety of microfluidic velocimetry techniques like micron-resolution Particle Image Velocimetry (μPIV), particle-tracking velocimetry (PTV), and others have been developed to characterize such microfluidic systems with spatial resolutions on the order of micrometers or less. This article discusses the fundamentals of established velocimetry techniques as well as the technical applications found in literature.

Keywords Micron-resolution particle image velocimetry (μPIV) · Microfluidics · Particle tracking velocimetry (PTV) · Microchannels

1 Introduction

Microfluidic velocimetry techniques such as micron-resolution Particle Image Velocimetry (μPIV) and particle tracking velocimetry (PTV) measure fluid motion in a spatially resolved manner with length scales ranging from 10^{-4} to 10^{-7} m. Fluid motion is observed through examination of tracer particles within the fluid. These particles are either artificially introduced into the fluid or are naturally occurring like red blood cells suspended within blood. Multiple experimental images are acquired and analyzed with particle tracking or spatial correlation methods to obtain the fluid's velocity from the displacement of the particles. μPIV refers to a microscopic adaptation of established macroscopic Particle Image Velocimetry (PIV) techniques. μPIV is regarded as independent from macroscopic PIV or PTV methods and has been widely accepted as a reliable microfluidic velocimetry technique.

Both microscale PIV and PTV techniques use tracer particles suspended in fluid, and a digital camera is used to acquire the location of suspended particles over time. PIV uses cross-correlation techniques to determine the particle displacement for an interrogation region within an image pair. High particle densities are usually a characteristic of PIV. PTV typically tracks single particles with nearest neighbor matching to determine particle displacement. In order to avoid particle misidentification, low particle seeding densities are common with PTV techniques. The appeal for high particle seeding density and avoidance of Brownian motion make PIV methods more desirable for nanoscale fluid mechanics.

Extensive reviews of PIV and PTV techniques and applications have been proposed by Adrian (1991, 1996, 2005), Raffel et al. (2007), Sinton (2004), and Lindken et al. (2009). Compared to macroscopic PIV, μPIV has considerably different optical and mechanical configurations. Fluorescent imaging is typically used to enhance the signal and overcome diffraction effects due to small particle size (<1 μm). The resolution can be improved to less than one micrometer with the use of a microscope equipped with proper optics. Volume illumination is used in μPIV, compared to light sheet illumination common in

S. J. Williams
Department of Mechanical Engineering, University of Louisville, 200 Sackett Hall, Louisville, KY 40292, USA

C. Park · S. T. Wereley (✉)
Birck Nanotechnology Center, Mechanical Engineering, Purdue University, West Lafayette, IN 47907, USA
e-mail: wereley@purdue.edu

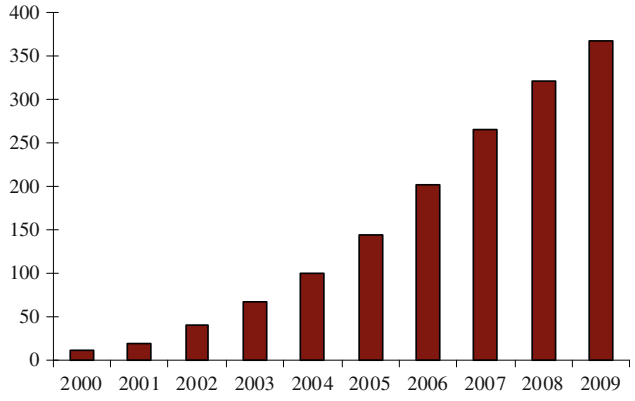

Fig. 1 Cumulative number of articles citing Santiago et al. (1998) through 2009

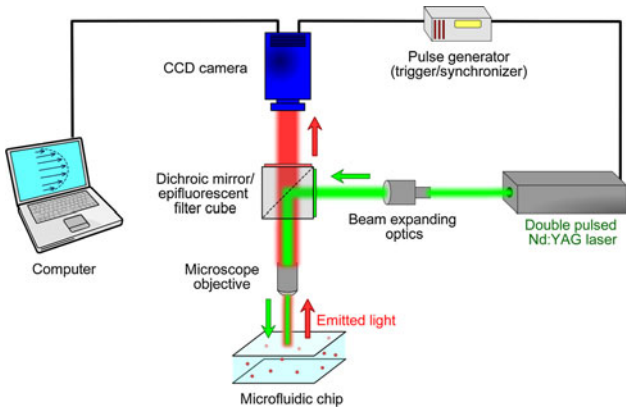

Fig. 2 Schematic of a traditional μPIV system

macroscopic PIV. These characteristics and additional considerations for traditional μPIV experimentation are discussed in the next section.

The μPIV technique that is commonly used in microfluidics was first introduced by Santiago et al. (1998) who determined fluid flow with spatial resolutions less than 10 μm. Using similar methods, a subsequent investigation by Meinhart et al. (1999) measured flow within a microchannel with spatial resolutions less than one micron. Since its inception, there have been many contributions and adaptations of μPIV. As of the beginning of 2010, the Santiago et al. (1998) article has been cited in journal articles 377 times according to a Web of Science® search (see Fig. 1). This article supplements the existing literature on the subject (Adrian 1991, 1996, 2005; Westerweel 1994; Sinton 2004; Raffel et al. 2007; Lindken et al. 2009). The fundamentals of traditional μPIV techniques are explained in Sect. 2. Novel adaptations and advancements of μPIV and 2D and 3D flow analysis are discussed in Sects. 3 and 4, respectively. Applications of these PIV techniques, including biologically relevant investigations, are discussed in Sects. 5 and 6. The information contained within this article will introduce the readers to available techniques and applications of μPIV, and to enable them incorporate one or more of the variety of techniques for their specific needs.

2 Overview of μPIV

A schematic of a typical μPIV setup is shown in Fig. 2. This setup consists of a microscope fitted with the proper optics, a microfluidic device, an illumination source, and an image acquisition system consisting of a computer and digital camera. Particles contained within the working fluid of the microfluidic device are excited with an external illumination source. The dichroic mirror filters the applied volume illumination and allows the emitted fluorescent light to pass toward the digital camera. Multiple particle images within the fluid are acquired with a digital camera and analyzed with a computer. The pulsed volumetric illumination source and digital camera shutter are synchronized, typically with a pulse generator. Not all microfluidic velocimetry systems are consistent with this illustration, the components within this system can be changed or modified to adapt to the needs of the experiment.

The microfluidic device is placed on the microscope stage to allow optical access to the microfluidic region of interest. Therefore, microfluidic devices incorporate a transparent window (typically glass) that forms one side of the contained fluidic channel. Another option is to fabricate the microfluidic device with a procedure called 'soft lithography' (Xia and Whitesides 1998) using poly(dimethylsiloxane), also known as PDMS. This material has been widely used to create microfluidic structures and has the added benefit of being optically transparent. Although transparent microfluidic devices are ideal for visual observation, μPIV techniques can be expanded for fluid investigations inside opaque devices, including silicon using infrared illumination (Han and Breuer 2001; Liu et al. 2005) or a wide array of substrates with X-ray illumination (Lee and Kim 2005, 2008b; Kim and Lee 2006). Components and characteristics of a traditional μPIV system are discussed in the following section, starting with volume illumination.

Turnkey μPIV systems are commercially available. TSI (www.tsi.com), Dantec Dynamics (www.dantecdynamics.com), and LaVision (www.lavision.de) are the main commercial suppliers of PIV systems and related equipment. The latter two companies currently do not supply their μPIV systems in the USA, as TSI holds the exclusive license to sell μPIV systems in the USA.

2.1 Volume illumination

One distinct difference between μPIV and macroscopic PIV is the nature of the illumination used to visualize and/or

excite the tracer particles. In macroscopic PIV, a sheet of light is used, defining the measurement plane. In μPIV, it is common to use volume illumination in which the entire depth of the test section is illuminated. The measurement plane in μPIV is defined by the depth-of-field of the recording lens. These measurement planes are sharply defined, allowing particles to transition quickly from being in focus to out of focus. The measurement depth for volume illumination has been calculated previously (Meinhart et al. 2000a; Olsen and Adrian 2000b) and was experimentally verified by Bourdon et al. (2004). The depth of correlation (DOC) is defined as the axial distance from the focused plane in which a particle becomes sufficiently out of focus, such that it does not significantly contribute to the correlation function. Initially focused particles that become out-of-focus in subsequent images produce unwanted noise and uncertainty. Analysis by Bourdon et al. (2006) showed that DOC is strongly dependent on numerical aperture (NA) and particle size, but weakly dependent upon objective lens magnification. The out-of-plane translation of tracer particles is influenced by Brownian motion (Olsen and Adrian 2000a), out-of-plane particle motion (Olsen and Bourdon 2003), and in-plane shearing (Olsen 2009).

Figure 2 represents the components of a typical μPIV system. The volume illumination originates from a double-pulsed laser system to generate monochromatic Nd:YAG laser light. The laser emits two pulses of 532 nm light with the duration of each pulse on the order of 10 ns. Optical components guide and expand the beam such that it can be applied broadly to the microfluidic device, exciting seeded fluorescent particles. A dichroic mirror allows the excited light to return to the objective and pass through to the camera while filtering out the laser illumination and background reflection, improving the signal-to-noise ratio of the acquired image. An interline-transfer charge-coupled device (CCD) camera is synchronized with the laser pulses to successfully obtain excited particle images. The interline-transfer feature of the camera allows the acquisition of an image pair to be recorded within $\sim$200 ns of each other. However, the frame rate for typical CCD cameras for continuous image acquisition is approximately 4–10 frames per second. In order to acquire images to observe transient microfluidic behaviors, a high-speed camera coupled with an appropriate light source should be utilized; a high-speed μPIV system as proposed by Shinohara et al. (2004) was able to acquire images at 500-μs intervals.

Alternatively, a broad spectrum white light source can be used (instead of pulsed light), such as a halogen lamp or mercury arc lamp. An excitation filter is used to allow a narrow wavelength band of light to excite the fluorescent particles. The shutter of the camera must be controlled to avoid over-exposed images which result in the formation of streaklines generated from the translation of the excited particles. Although streaklines give insight into the direction of fluid flow, they need to be avoided for subsequent μPIV image processing. Continuous illumination is sufficient for some microfluidic applications, but the dual-pulsed laser illumination synchronized with a CCD camera can rapidly capture image pairs, enabling observation of faster flows. For example, with pulsed laser illumination Meinhart et al. (1999) was able to measure fluid velocities three orders of magnitude greater than the initial effort by Santiago et al. (1998) who used continuous illumination.

Dark field illumination enables the application of non-fluorescent cells and other unstained micro-organisms as tracer particles. Diffracted light (as opposed to incident light) passes through a small objective aperture in the objective lens' back focal plane. Malsch et al. (2008) used yeast ($\sim$4 μm diameter) to investigate fluid motion within droplets of water. The illumination scheme involved a red high powered LED and a 10× objective lens (NA 0.2). Dark field images are typically clear of artifacts; however, due to low light levels in the acquired image proper interpretation of these images is important.

Another potential illumination scheme utilizes evanescent waves (EWs) (Zettner and Yoda 2003), this technique is discussed further in Sect. 3.1.

2.2 Particles

Fluorescent tracer particles used in μPIV are typically ranging from 200 nm to 1 μm. These particles are small enough to follow fluid flow, but they need to be large enough to scatter sufficient light for the recorded images. Spatial resolution can be further improved if high NA, diffraction-limited optics are used to resolve the imaged particles at least to the extent of 3–4 pixels per particle. Fluorescently labeled particles are commercially available in a wide variety of diameters. Companies like Thermo Scientific, Sigma-Aldrich, Polysciences Inc., and Spherotech offer a variety of microparticles in sizes ranging from 20 nm to 1.0 mm typically composed of polystyrene, latex, and silica. These tracers are available in a variety of excitable wavelengths; alternatively, metallic, magnetic, or dyed non-fluorescent particles are available.

The amount of scattered light from a particle decreases as the diameter of the fluorescent particle decreases; for particle diameters much smaller than the wavelength of light, the amount scattered by a particle varies as d^{-6} (Born and Wolf 1999). Quantum dots have been applied to μPIV and overcome limitations of fluorescent particles of similar size as their excitation band is very broad and the emission is independent of excitation wavelength (Pouya et al. 2005). Quantum dots are quite small (10–50 nm). Their size regulates the band of emitted light, and they are not susceptible to photobleaching. However, owing to their

small size, the obscuring effect of Brownian motion becomes more apparent. Freudenthal et al. (2007) was able to attach quantum dots to a larger 70-nm particle, enabling the benefits of quantum dots while dampening Brownian motion. Guasto et al. (2006) developed a statistical approach to tracking Quantum dots and other nanometer-sized particles due to their high diffusivity and fluorescence intermittency. By means of tracking single quantum dots, near-wall fluid velocity and temperature have been measured (Guasto and Breuer 2008).

The tracer particles themselves do not have to be fluorescently tagged, nor rigid spheres. For example, a number of experimenters (Sugii et al. 2002; Bitsch et al. 2003; Park et al. 2004a) have used red blood cells as tracers in μPIV analysis. Red blood cells themselves have been fluorescently labeled for fluid velocimetry investigations (Ravnic et al. 2006). These and other 'non-traditional' velocimetry methods are discussed in Sect. 3.

2.3 Brownian motion

Brownian motion is the result of random thermal noise in the fluid. It can cause error in the measurement of the flow velocity due to the uncertainty in the location of the particle. The source of error was quantified by Santiago et al. (1998) relative to the displacement of the particle. This random motion is related to the diffusivity of the particle: displacement increases as the particle diameter decreases and as temperature increases. Owing to the obscuring effects of Brownian motion, this will set a lower limit for the size of the particle to be used in μPIV for a given flow speed. The relative error (ε) due to imaging the random particle displacement is given as

$$\varepsilon = \frac{1}{u}\sqrt{\frac{2D}{\Delta t}}$$

where u is the time-averaged local fluid velocity for a period of time (Δt), and D is the diffusivity of the particle. Brownian motion causes a broadening of the correlation signal peak (Olsen and Adrian 2000a). This effect is relatively less important for faster flows. Also, since this effect is due to random motion, this error can be reduced by imaging several particles in a single interrogation window, and by ensemble averaging over many images. Recently, Olsen and Bourdon (2007) produced advanced simulations of Brownian motion to predict the experimental error in PIV experiments.

Even though Brownian motion may be an obscuring effect for fluid velocimetry measurements, it has been used constructively to characterize diffusivity-related properties of the particle. Since the severity of Brownian motion is a function of temperature, particle translational data can be used to produce temperature measurements (Hohreiter et al. 2002; Chamarthy et al. 2009). Gorti et al. (2008) used Brownian motion to measure the diffusivity of particles to monitor the adhesion of viruses to an antibody-coated polystyrene microparticle. They found that the attached viruses increased the drag coefficient of the particle, decreasing the effect of Brownian motion.

2.4 Image processing

Digital μPIV recordings are evaluated with conventional correlation-based algorithms. A sufficient number of particle images are required in the interrogation window for reliable and accurate measurements. The advantage of analyzing microfluidic flows is that the fluid mechanics are often simplified to steady, quasi-steady or periodic due to very low Reynolds numbers (usually less than one), resulting in a laminar, Stokes flow regime. Typically, velocity vectors are obtained through spatial cross-correlation of the image pairs (Keane and Adrian 1992). Computation time is significantly reduced through fast Fourier transform-based cross-correlation calculation (Willert and Gharib 1991).

Owing to the laminar and steady nature of microfluidic flows, many image pairs can be analyzed with a correlation technique termed ensemble averaging or correlation averaging (Meinhart et al. 2000b). This technique enhances the acquired signal by reducing the negative influences of Brownian motion, low seed particle concentration, and low-quality images (Meinhart et al. 2000b; Wereley et al. 2002; Devasenathipathy et al. 2003). Many image pairs, typically hundreds of them, can be averaged to significantly increase the signal-to-noise ratio of the measurements. If the flow is neither steady state nor periodic, then the velocimetry analysis is restricted to only one image pair for that instant in time. These measurements may contain vectors that deviate in magnitude and direction from nearby vectors. A statistical model that detects such spurious vectors has been described by Westerweel (1994).

From the many image pairs obtained, background noise can be readily removed. One method is to average all of the images to produce a background image (Gui et al. 1997b); particles move through the region quickly, minimally affecting the averaged images. Another method is to obtain the minimum gray value at each pixel for the ensemble of PIV images (Cowen and Monismith 1997). For either case, the resulting background can be subtracted from the recordings. Another source of error is associated with the out-of-plane motion of particles. Olsen and Bourdon (2003) analyzed this source of error, with one result being that the magnitude of the PIV signal peak from correlation will decrease. This source of error is significantly reduced with correlation averaging and removing background noise. Advanced algorithms including second-order central difference interrogation (CDI), central difference image

correction (CDIC), and continuous window shift (CWS) have been used in μPIV analyses and are discussed in detail elsewhere (Cowen and Monismith 1997; Gui et al. 1997a; Huang et al. 1997; Gomez et al. 2001; Wereley and Meinhart 2001; Wereley et al. 2002; Wereley and Gui 2003).

Typical cross-correlation requires two multi-pixel interrogation windows to calculate one velocity vector. The first window defines the resolution of the velocity measurement. The second window is offset from the first and is large enough to contain image information from the first window. Larger windows contain more particle images, but will lower measurement resolution and produce errors from velocity gradients within that window. In theory, interrogation regions can be reduced to one pixel. A single pixel evaluation (SPE) algorithm for μPIV was proposed by Westerweel et al. (2004) to drastically improve the spatial resolution without decreasing the signal-to-noise ratio. In SPE, the interrogation window is shrunk to one pixel while information is gathered by varying the second pixel location within a specified radius. A much larger number of image pairs are necessary with SPE compared to standard cross-correlation methods. SPE methods have been the recent focus for μPIV investigations (Wereley et al. 2005; Chuang and Wereley 2007).

Although traditional μPIV techniques have been implemented in a variety of microfluidic flow field investigations, it has its distinct limitations. First, these measurements are typically two-dimensional, two-component (2D–2C) meaning that out of plane velocity components are not measured. Second, the fluid flow needs to be steady state or periodic such that a sufficient number of image pairs can be acquired to eliminate sources of measurement error such as Brownian motion. Third, one surface of the system under investigation needs to be transparent such that fluorescent tracer particles can be excited and recorded—this becomes more challenging with opaque devices. In order to overcome these limitations, innovative PIV and PTV techniques have been developed and will be discussed in the later sections.

3 Related microfluidic velocimetry techniques

3.1 Evanescent wave μPIV

An EW is a near-field standing wave generated by total internal reflection (TIR) at the interface between two transparent media of different refractive indices when the incident angle of the light is greater than the critical angle. EW illumination has been widely adopted in μPIV to achieve higher spatial resolution, even as the dimensions of the tracer particles and microchannel are less than one micron. However, its illumination is confined within several hundred nanometers from the microchannel wall, as the intensity of EWs decay exponentially with the distance from the interface from which it occurs. Thus, EW μPIV was often used to investigate the near-wall velocity profile in a microchannel (See Fig. 3). EW μPIV was first proposed by Zettner and Yoda (2003) and used to measure the near-wall velocity profile of creeping rotating Couette flow within 380 nm from the channel wall. The small penetration depth (50–250 nm) of EW reduced background noise resulting from the out-of-focus tracer particles. Jin et al. (2004) analyzed images of sub micron particles (200 nm and 300 nm diameters) with a particle tracking velocimetry algorithm to extract information about apparent slip velocity. Li et al. (2006) extended EW μPIV for multilayer velocity measurements, as particles closer to the channel wall experience greater intensities. However, tracer particles can readily move out of the illuminated area due to Brownian motion effects, which causes severe particle mismatch when performing a cross-correlation (Sadr et al. 2004, 2005, 2007; Hohenegger and Mucha 2007). Despite this restriction, EW μPIV is valuable in determining fluid interactions with the channel wall.

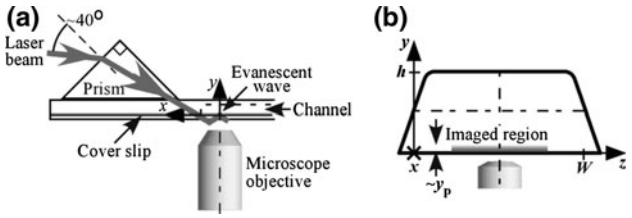

Fig. 3 μPIV using evanescent wave illumination. **a** Schematic illustration of how evanescent wave can be produced from a prism; **b** Evanescent wave region on the bottom wall of a microchannel. From Sadr et al. (2004), with permission

3.2 X-ray μPIV

X-rays are electromagnetic radiation and primarily used for medical diagnostic imaging due to their penetrating property. Since many microfluidic chips contain transparent materials (glass, PDMS) and fluids, traditional μPIV is commonly used. However, a μPIV technique using a coherent synchrotron X-ray beam as a light source can be very useful in a variety of applications, including flow inside an opaque microchannel. X-ray μPIV can be used for measuring volumetric flow rate, since all particles passing through the pathway of the X-ray beam are imaged in an opaque material (Lee and Kim 2003). This technique was employed to investigate blood flow in an opaque tube through the analysis of the fringe patterns of red blood cells (Lee and Kim 2005; Kim and Lee 2006; Dubsky et al. 2008). In addition, X-ray μPIV with multiple projections was proposed not only to improve the accuracy of velocity

profile but also to obtain 3D–3C measurement (Dubsky et al. 2008). For visualization, X-rays were converted to visible light by passing them through a thin $CdWO_4$ scintillation crystal. Although this is a valuable technique for biological flows and opaque devices, it needs to be carefully implemented and optimized to prevent excessive radiation exposure.

3.3 IR μPIV

Infrared (IR) radiation is electromagnetic radiation with a wavelength longer than visible light and is transmitted through silicon with very little absorption. Similar to X-rays, IR μPIV can be applied to measure the velocity profile within silicon microchannels. Conventional tracer particles do not emit and absorb in the IR regime, and the wavelength and tracer particle diameter needs to be chosen to maximize scattering intensity (Han and Breuer 2001). The very high index of refraction of silicon ($n = 3.3$) will also distort the image. Therefore, the spatial resolution of IR μPIV is not as good as that of the conventional μPIV (Han and Breuer 2001; Liu et al. 2005). IR μPIV was applied to investigate flow around a heat sink (Jones et al. 2008), and the images were processed with an algorithm that was developed to improve the quality of IR recordings.

4 Three dimensional techniques

4.1 Confocal μPIV

Owing to high particle density and volume illumination, additional interference is introduced from light emitted from neighboring fluorescent particles. Confocal μPIV was applied to improve image contrasts, leading to more accurate vector fields. The advantage of confocal μPIV is the significant reduction of out-of-focus light. It is as if thin light sheets were extracted from the illuminated volume. However, traditional confocal imaging has slow scanning rates. Tanaami et al. (2002) developed a high-speed confocal scanner capable of acquiring images once per millisecond. Park et al. (2004b) adapted this system for μPIV applications and later applied it to investigate the flow between stationary and rotating disks kept 180 μm apart (Park and Kihm 2006b). This laser-based system included a microlens disk and pinhole array disk spinning in unison. An illustration of this system is shown in Fig. 4. The pinhole aperture allows the emitted fluorescent light exclusively from the focal plane to pass through and blocks out fluorescent light emitted from outside the focal point. The rotating microlens array allows light to be delivered throughout the depth of the experimental area, enabling three-dimensional, two-component (3D–2C) flow field

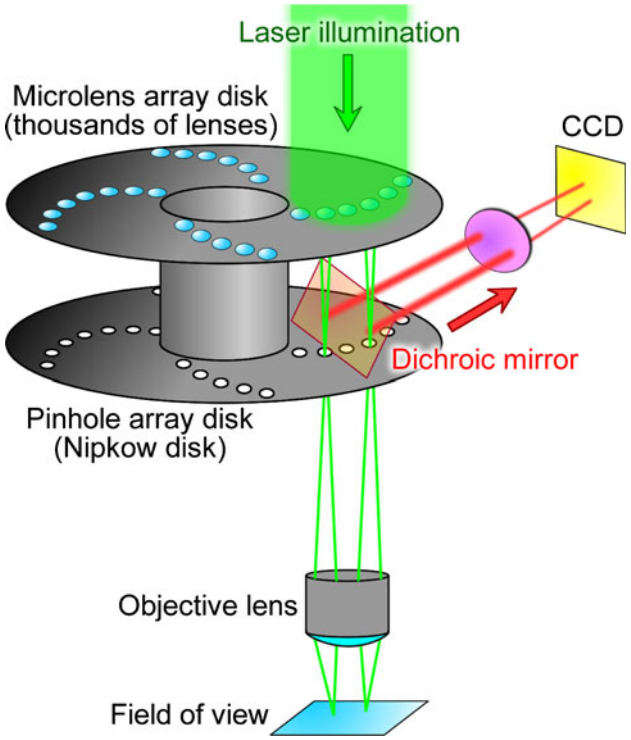

Fig. 4 Design for high-speed confocal laser scanning microscopy. After Park et al. (2004b) and Lima et al. (2006)

analysis. A high-speed confocal scanner developed by Kinoshita et al. (2007) was capable of scanning at 2000 fps enabling the analysis of fluid motion within a droplet at 9.1-μm resolution and a confocal depth of 1.88 μm.

Confocal μPIV is limited to steady flows as it takes a relatively long time to adequately scan the depth of the investigated region. The analyzed image planes result in 3D–2C measurements. The improvement in image contrast is shown in Fig. 5, comparing experimental images acquired with confocal μPIV and traditional, volume illuminated μPIV. Lima et al. (2006, 2007, 2008a, b) applied confocal μPIV to investigate the flow of red blood cells within a microchannel with Reynolds numbers up to 0.1. Confocal microfluidic velocimetry techniques have been applied to simultaneously measure pH with an uncertainty of 0.23 using a pH-sensitive fluorescent dye (Ichiyanagi et al. 2007).

4.2 3D–3C μPIV analysis

From 3D–2C velocity measurements, the out-of-plane velocities of the fluid can be determined analytically on application of the continuity equation (Robinson and Rockwell 1993). Coupled with microfluidic velocimetry techniques, this analysis results in 3D–3D velocity distribution with micron spatial resolution. For steady flows, 3D velocity distributions can be obtained from a set of 2D–2C

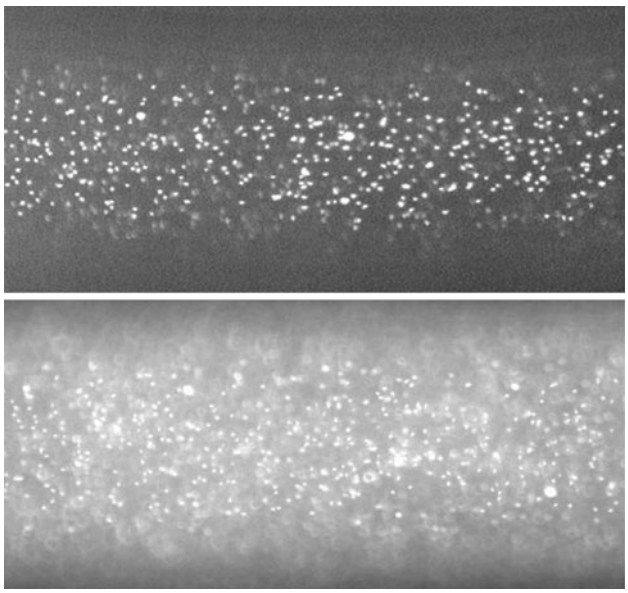

Fig. 5 Particle images acquired using confocal microscopy (*top*) and conventional volume illuminated microscopy (*bottom*). From Park et al. (2004b) with permission

data of field layers that are spaced at a known distance apart in the out-of-plane direction. Confocal velocimetry techniques obtain 3D–2C information of fluid motion. 3D velocity data are calculated by integrating the continuity equation in the out-of-plane direction. However, one must know a boundary condition or plane of symmetry to begin the integration. Pommer et al. (2007) applied this technique to the flow around an adherent red blood cell to investigate applied fluid shear forces, and the out-of-plane velocimetry results had an uncertainty of 3% of the free stream velocity. Adaptation of this analytical technique toward a precise piezo-electric confocal microscopy system results in out-of-plane velocity errors equivalent to that of the of the in-plane components (Kinoshita et al. 2007).

An alternative method to obtain 3D–3C velocimetry involved a modification of a macroscale technique that correlated images of particles between two light sheets (Raffel et al. 1995) and adapted it toward volume illumination typical of μPIV (Shinohara et al. 2005). This technique determines the 3D position of tracer particles as opposed to calculating the out-of-plane fluid velocity vectors from PIV measurements. Additional 3D microfluidic PIV and PTV techniques are discussed in the following sections.

4.3 Stereoscopic μPIV

In stereoscopic μPIV, two cameras are used to view the same experimental area from two different viewing angles as opposed to previous single-camera methods. Simultaneous images are acquired and analyzed based on separate calibration, resulting in reconstruction of 3D velocity components over a planar region (2D–3C). Stereoscopic PIV has been applied to macroscopic fluid flows (Prasad and Adrian 1993), and systems are commercially available. However, there were fundamental challenges applying stereoscopic PIV to microfluidics, especially in adapting multiple camera angles with microscopic imaging techniques. Klank et al. (2002) obtained velocity components over a 16-μm-thick plane of flow inside a cell sorter. The accuracy of the out-of-plane velocities was limited to the small difference between the two camera angles (<6°). Lindken et al. (2005, 2006) were the first develop a stereoscopic μPIV system (Fig. 6). They were able to obtain a full 3D velocity map of a T-shaped micromixer by investigating multiple scanned planes. Although their angle between the two cameras was at 27.5°, large for stereoscopic μPIV, the authors considered this a limiting factor in the accuracy of the out-of-plane velocity components. One limitation is that stereoscopic μPIV requires objectives with low NA and large depth-of-field as opposed to high NA lenses associated with traditional μPIV. Further, the accuracy of correlation-based measurements is limited by the overlap between of the two imaged fields (Bown et al. 2006). Hagsater et al. (2008) proposed a configuration containing reflective prisms placed between the fluid system and the objective lens with both views imaged with a single camera, offering an innovative alternative to multi-camera stereoscopic analysis.

4.4 Digital holographic μPIV

A hologram contains both amplitude and phase information of an object instead of simply traditional intensity data. A holographic image of tracer particles contains 3D

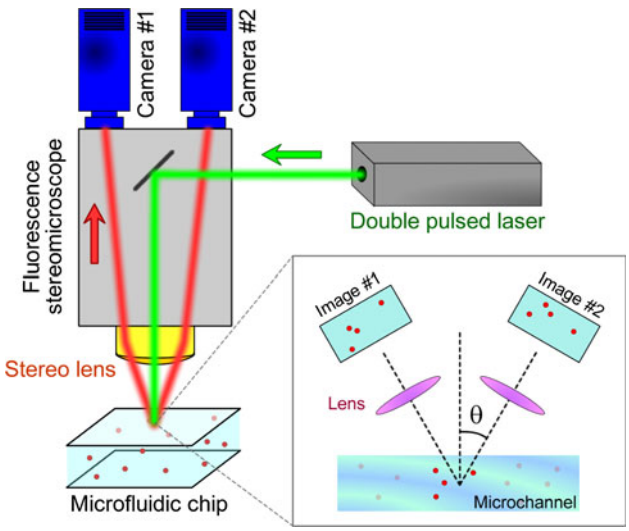

Fig. 6 Schematic diagram of stereoscopic μPIV

information about the recorded object. Digital holography utilizes a CCD camera instead of holographic films or plates to record holograms. Satake et al. (2005, 2006) was the first to apply this technique to track particles for microfluidic velocimetry. They acquired images at a rate of 1 kHz measuring the flow within a 92-μm capillary. An illustration of their experimental procedure as well as a holographic image of microparticles is shown in Fig. 7. Typically the particles are seeded at a low density to prevent them from optically interfering with each other. Sheng et al. (2006) used a higher density of particles with higher hologram magnification. They were able to image 2000 particles per cubic millimeter (10× objective) as well as visualize sub micrometer particles (0.75 μm, 40× lens). With a high speed camera they were able to resolve the location of several thousand particles and measure their 3D trajectories. Lee and Kim (2008a) applied digital holographic techniques for particle tracking velocimetry (PTV) to measure flow within a curved microchannel with a circular cross section. They obtained over 4000 instantaneous velocity vectors during a 1-s period by tracking the 3D locations of particles from reconstructed holograph images. Holographic methods show promise in obtaining 3D–3C microscale flow measurements, yet extensive image processing and reconstruction is necessary to implement this technique. In addition, like most PTV methods, a high tracer particle density leads to interference from neighboring particles leading to increased measurement error.

Holography has been integrated with optical trapping techniques, yielding highly configurable optical landscapes capable of trapping and precisely positioning over one hundred individual suspended particles (Grier 2003). Di Leonardo et al. (2006) combined holographic optical trapping with traditional microparticle tracking techniques for multipoint measurements of flow fields. Optical trapping forces rigidly held suspended particles against fluid motion. Then, the optical traps were briefly deactivated, the fluid carried the released particles from their initial position, and the images were acquired to determine particle translation as a function of time. Optical traps were reactivated, recapturing the tracked particles to their initial position. With particle tracking velocimetry, the velocities of each trapped and released particle were calculated. This technique requires a smaller amount of probe particles compared to traditional μPIV and PTV techniques. The optical trapping system limits the number of simultaneous particles used and the trap strength limits the maximum velocity of the fluid. The advantage of implementing this technique is that it provides precise placement of tracer particles to the region of interest, as long as the strength of the optical trap can hold the tracer particle against bulk fluid drag forces.

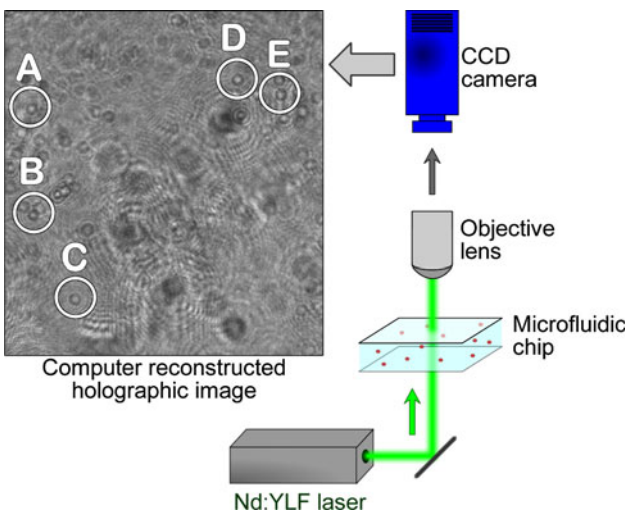

Fig. 7 Experimental setup for digital holographic micro particle velocimetry and a holographic image with five arbitrary microparticles labeled. After Satake et al. (2006)

4.5 Defocused techniques

There are two defocusing techniques that have been used to track the three-dimensional translation and velocity of individual particles. Fluid velocimetry is obtained through particle tracking techniques, as opposed to image correlation commonly associated with μPIV. The first technique uses a single camera system in conjunction with a mask (three pin holes) embedded in the camera lens to create triangular particle image patterns from the fluorescent particles (Willert and Gharib 1992). The sizes and locations of the particle image patterns on the image plane relate directly to the three-dimensional positions of the individual particles. A calibration step is necessary to extract out-of-plane data from acquired images. Yoon and Kim (2006) adapted this method to measure microfluidic flows over a backward-facing step; they achieved a 1-μm out-of-plane resolution and a 5-μm in-plane resolution. A schematic diagram of the defocusing concept and their acquired calibration images are shown in Fig. 8. Pereira et al. (2007) applied this technique to track the complex 3D motion of tracer particles within an evaporating water droplet. Difficulty arises in discerning the nature of overlapping triangular particle images. Alternatives to overcome this hindrance include having color-filtered pinholes (Tien et al. 2008) or replace the three-hole aperture with an annular aperture (Lin et al. 2008).

The second defocusing technique extracts 3D position data using information encoded in the ring structure of a defocused particle image. A fluorescent particle smaller than the diffraction limit for the imaging system being used creates a ring pattern that is a function of its distance from the focal plane. The outermost ring diameter and image

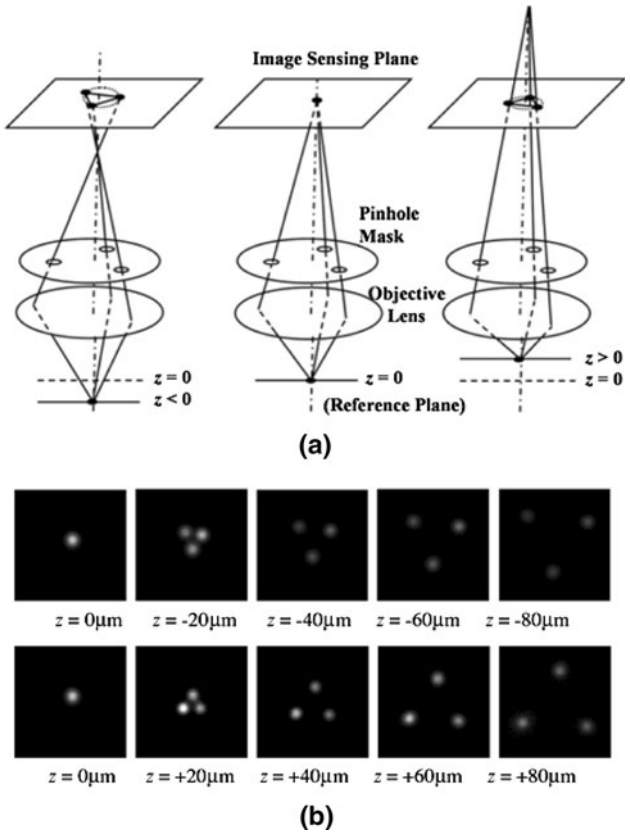

Fig. 8 **a** Schematic diagram and **b** calibration images for the defocusing concept using a three pin hole mask. From Yoon and Kim (2006), with permission

pattern gives information that can be applied to individual tracking of fluorescent micrometer particles (Speidel et al. 2003; Wu et al. 2005). An algorithm has been developed, which applied this technique for 3D particle tracking (Park and Kihm 2006a; Peterson et al. 2008). A calibration curve regarding the relationship of the defocused particle image with a known out-of-plane distance is obtained prior to experimentation. This calibration curve is used to extract 3D position and velocity data from acquired experimental particle images. Low particle density was used to prevent optical interference from neighboring defocused particle images. Figure 9 shows acquired images used to calibrate

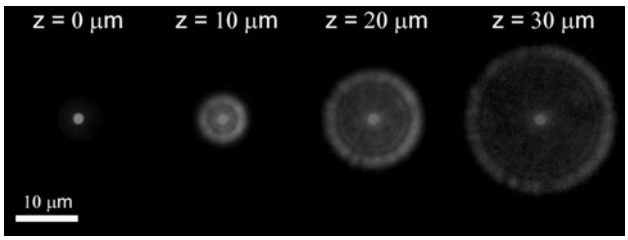

Fig. 9 Calibration images of defocused 3.0 μm particles with a 60× water immersion lens (Peterson et al. 2008)

the out-of-plane distance of defocused particles (Peterson et al. 2008).

5 μPIV applications

5.1 Near-wall and slip velocity

One of the first applications of μPIV was the measurement of the velocity profiles within a microchannel. A spatial resolution of 0.9 μm was achieved in a glass rectangular microchannel of 30 μm (depth) × 300 μm (width) × 25 mm (length) and the near-wall fluid velocity was obtained within 450 nm of the wall (Meinhart et al. 1999). Tretheway and Meinhart (2002) described the effect of surface properties such as hydrophobicity and hydrophilicity on the velocity profiles within 450 nm of the microchannel. The measured slip velocity on hydrophobic surface was approximately 10% of the free-stream velocity while the velocity on hydrophilic surface was in agreement with the no-slip boundary condition. Fluid slip at micron and nanometer length scales was also discussed. Tretheway and Meinhart (2004) extended their previous work to investigate fluid slip, especially for hydrophobic surfaces. They concluded that either an effective air gap due to a depleted water layer or nanobubbles were related to fluid slip. A similar study has also been done by using hydrophobic glass surface which was grafted with a monolayer of silane. Joseph and Tabeling (2005) used a high NA objective (1.3) to remove out-of-focus tracers and imaged particles within 0.5 μm of the wall of a microchannel (10 μm × 100 μm × 1 cm) fabricated from PDMS and glass and reported that the slip length was less than 100 nm. Kähler et al. (2006) measured the near-wall velocity profiles in three types of fluid flow (laminar, transitional, and turbulent flow) and proposed several techniques to achieve high accuracy and spatial resolution. Zhu et al. (2005) proposed 3D simulation model for fluid slip phenomena in hydrophobic microchannels by using the lattice Boltzmann method, and compared this with experimental μPIV results. They concluded that the fluid slip on the side walls was approximately 9% of the main stream velocity. Karri et al. (2009) introduced a method for improving the estimation of near-wall velocity gradients from noisy flow data using Gaussian and generalized multiquadratic radial basis functions to optimize fitting parameters. This method improved accuracy by 10-15% and reduced computation cost by approximately 75%. Evanescent wave μPIV (Sect. 4.2) is able to reduce noise from fluorescent particles not close to the channel wall. The illumination intensity decays from the wall as $1/e$, restricting the region illuminated by the EW to be within a few hundred nanometers. Zettner and Yoda (2003) obtained velocity data within 380 nm of the channel wall.

5.2 Electrokinetics

Recently, μPIV has been widely used to determine the velocity profiles of electrokinetically induced particle movement and fluid flow. Besides hydrodynamic drag, many electrokinetic phenomena can influence particle motion including dielectrophoresis and electro-osmosis. It is, therefore, important to develop techniques to accurately determine electrokinetic particle motion and distinguish it from fluid velocimetry. Devasenathipathy and Santiago (2002) proposed a μPIV method to investigate electro-osmotic flows. This method involved particle calibration experiments to determine the electrophoretic mobility of tracer particles and measuring the channel wall zeta potential. This calibration allowed for the determination of true flow measurements. The electrokinetic response of different sized particles will differ, and microfluidic motion can be determined through PIV measurements of both particles (Meinhart et al. 2003). Wang et al. (2005) proposed a technique called two-color μPIV with two different particle sizes to accurately measure the velocity profiles of fluid in the presence of an electric field. The two different sized particles exhibit different electrokinetic forces and, through electrokinetic scaling laws, accurate fluid velocity could be determined. This technique was used to analyze electrokinetic fluid and particle motion within a wedge-shaped microchannel. Two-color μPIV was also applied to investigate the concentration of DNA with AC electro-osmotic pumping (Brown and Meinhart 2006). Sadr et al. (2004, 2006) measured the velocity profiles of fully developed, steady flow induced by electro-osmosis. In a rectangular channel, a steady electric field up to 4.8 kVm^{-1} was applied to a diluted borax solution of different concentrations, and the induced electro-osmotic flow was analyzed using μPIV with EW illumination. Thus, the near-wall velocity profile was obtained within 100 nm of the channel wall. Fluorescent dye has been combined with μPIV to evaluate mixing efficiencies for the electro-osmotic flow (Ichiyanagi et al. 2009). Kumar et al. (2008) generated and analyzed optically induced electrothermal microfluidic vortices, created through simultaneous application of a focused laser beam and an alternating current (AC) signal. The microchannel consisted of parallel glass plates coated with indium tin oxide (ITO) and separated by 50 μm. The velocity profile of vortex flow in the focal plane was measured by μPIV. Lu et al. (2008) measured the velocity profiles across a moving droplet actuated by electrowetting-on-dielectric (EWOD). The 3D flow field of an EWOD actuated 0.1 μl droplet translating at 2 mm/s was calculated from multiple μPIV-acquired planar 2D flow fields. Microfluidic velocimetry techniques have been applied to investigate a variety of electrohydrodynamic mechanisms. However, the particles themselves will be altered by the applied electric field. Future integration of velocimetry techniques into electrokinetic investigations need to account for particle electrokinetics, which is why techniques like two-color μPIV are valuable for future electrokinetic flow characterization.

5.3 μPIV thermometry

μPIV can be used to measure the temperature of the fluid through the analysis of the Brownian motion of the tracer particles. As temperature increases, the Brownian motion of a particle also increases. Changes in Brownian motion can be detected from the correlation peak resulting from a spatial cross-correlation algorithm (Hohreiter et al. 2002; Chamarthy et al. 2009). Greater Brownian motion results in the broadening of the correlation peak. Temperature (T) can be determined through the mean square displacement of a particle:

$$\left\langle s^2 \right\rangle = 2D\Delta t = \frac{2k\Delta t}{3\pi d_p} \cdot \frac{T}{\mu}$$

where k is Boltzmann's constant, μ is viscosity, and d_p is the particle diameter. The temperature in the range of 20–80°C for stationary water was experimentally detected within the average uncertainty of ±3°C using μPIV. In addition, it is reported that both velocity and temperature can be simultaneously measured for water when the fluid velocity is less than or equal to 8 mm s^{-1} and the temperature is greater than 20°C (Hohreiter et al. 2002). Park et al. (2005) used Optical Serial Scanning Microscopy (OSSM) to measure the 3D Brownian motion and deduced temperature information with uncertainties of 5.54%, 4.26%, and 3.19% in the 1D, 2D, and 3D cases, respectively. Kihm et al. (2004) used EWs to monitor the 3D Brownian displacement of 200 nm particles near a wall. Measurements in the lateral direction were in agreement with theory, yet the out-of-plane discrepancies were attributed to potential electrokinetic interactions with the wall.

Thermochromatic liquid crystals (TLC) are capable of displaying different colors at different temperatures (Csendes et al. 1996; Fujisawa et al. 2005). Microencapsulated crystals are in the range of (10–25 μm) and can be implemented with PIV techniques for simultaneous temperature and velocimetry measurements (Dabiri 2009). However, their relatively large diameters inhibit their use in sub-100-μm microfluidic investigations (Muwanga and Hassan 2006).

Laser-Induced Fluorescence (LIF) is capable of making non-invasive temperature measurements within a volume of fluid. A temperature-dependent fluorescent dye (typically Rhodamine B) is either calibrated (Ross et al. 2001) or normalized with a temperature-independent dye

(typically Rhodamine 110) for two-color LIF (Sakakibara and Adrian 1999; Kim and Kihm 2002; Ross and Locascio 2003; Natrajan and Christensen 2009). Sakakibara and Adrian (1999) have claimed an accuracy of ±0.17°C with two-color LIF. Instead of injecting the dye into the microfluidic device, the surface of microchannel can be coated with a film of temperature-dependent dye. With this technique, Sato et al. (2004) achieved temperature resolution of 0.26 K with a μPIV measurement resolution of 5 μm by 5 μm.

5.4 Other applications

μPIV has been combined with other methods, resulting in interesting applications. μPIV can be used to characterize the fluid flow within biochips; Gomez et al. (2001) made a microelectronic, microfluidic device which can measure the electrical impedance of microorganisms like Listeria innocua. Simultaneous μPIV and impedance measurements enable simultaneous fluid characterization and real-time monitoring of biological species. The combination of μPIV and optical tweezers (called μPIVOT) was proposed to measure the velocity profile around a trapped suspended particle, which would provide clues toward a better understanding of biological cells suspended in a fluid medium (Neve et al. 2008). It was reported that when the trapped particle with diameter between 15 and 35 μm was exposed to fluid flow from 50 μm s^{-1} to 500 μm s^{-1}, the influence of optical tweezers acting on the tracer particles can be neglected.

Through coupling a pressure transducer with μPIV, the pressure gradient and velocity profile were determined to measure the viscosity of *E. coli* DNA solution (Curtin et al. 2006). This technique does not require the extraction of a fluid sample and can be classified as a zero-volume viscosity measurement technique. Wang et al. (2007) investigated the recirculating flow inside a droplet and characterized the mixing of two aqueous droplets by using μPIV. In each case, a carrier fluid of oil was used with a de-ionized water droplet (Fig. 10)—results allow a better understanding of droplet mixing for the development of future droplet-based lab-on-a-chip devices. Droplet-based microfluidic devices enhance and accelerate chemical and biological processes, offer miniaturized compartmentalization, and provide precise control of volumes (Song et al. 2006). A μPIV technique was used to measure the velocity profile within an inkjet printhead (Meinhart and Zhang 2000). The importance of this investigation was, for the first time, μPIV was used to measure instantaneous flow inside a commercially available inkjet printhead. Similar techniques could be used to characterize manufactured microfluidic devices.

Mixing and separation is an important and well-documented topic in microfluidics (Squires and Quake 2005). Velocimetry techniques have been integrated with these systems to characterize their behavior at this scale. Mixing of a fluorescent dye into a non-fluorescent stream can be easily visualized, yet the simultaneous incorporation of μPIV can yield valuable velocimetry measurements (Sato et al. 2004; Hoffmann et al. 2006). Stereoscopic techniques have enabled 3D–3C velocimetry measurements to characterize mixing within microchannels (Lindken et al. 2005, 2006). Alternatively, mixing can be quantified through measuring the effective diffusion coefficient of tracer particles. Kim and Breuer (2007) coated a microchannel with bacteria to enhance mixing and determined the diffusion coefficient through particle-tracking velocimetry to measure tracer particle displacement. These are just a few examples exhibiting the implementation of various velocimetry techniques to characterize mixing, and these techniques will continue to play a vital role in the analysis of microfluidic phenomena and device performance.

6 Biological application of μPIV

Proper characterization of biological flows, whether it is the velocity of red blood cells through a developing

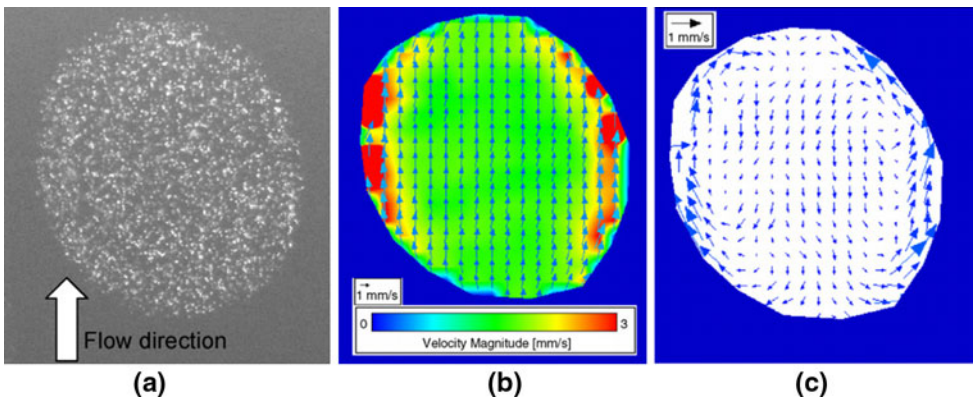

Fig. 10 μPIV results of the velocity distribution inside a moving droplet (DI water) in a carrier fluid (oil). **a** μPIV image and velocity distributions relative to **b** a fixed reference and **c** a moving droplet. From Wang et al. (2007), with permission

embryo or fluid interactions with oceanic phytoplankton, is important for the basic understanding for physiological or biological systems as well as the development of the next generation medical devices. Microscale biological fluid flow investigations are a relatively unknown area due to the distinct challenges limiting the implementation of PIV techniques for such analyses. This section provides specific examples of how some of the previously mentioned velocimetry techniques have been used for analysis of biological flows.

6.1 Blood flow

μPIV has commonly been employed as a tool for investigating flow phenomena occurring in many micro-channel structures, especially in the field of biological experiments. Investigation of in vivo and/or in vitro blood flow has been widely explored by many researchers with various techniques, including conventional μPIV (Sugii et al. 2002; Bitsch et al. 2003, 2005; Vennemann et al. 2005, 2006; Poelma et al. 2008), X-ray μPIV (Lee and Kim 2005, 2008b; Kim and Lee 2006), and confocal μPIV (Lima et al. 2007, 2008a, b). μPIV gives more detailed information about the biomechanics of blood microcirculation since: for example, reasonably high spatial resolution in μPIV allows the estimation of wall shear stress from the accurate velocity measurement (Vennemann et al. 2007). In order to quantitatively measure blood flow, red blood cells (Sugii et al. 2002; Bitsch et al. 2003, 2005; Lee and Kim 2005; Kim and Lee 2006; Lee et al. 2007; Lima et al. 2008a), and fluorescent particles (Vennemann et al. 2005, 2006; Lima et al. 2007, 2008b; Poelma et al. 2008) are often used as tracer particles.

6.1.1 RBCs and platelets as tracer particles

In order to measure the velocity field of blood flow in the arteriole of the rat mesentery, a μPIV technique was employed while using RBCs as tracer particles (Sugii et al. 2002). The movement of the mesentery was also measured and considered to improve the accuracy of the RBC velocity measurements. The displacement of the mesentery and its velocity are in the ranges from −1.9 to 1.6 μm and −0.26 to 0.17 mm s^{-1}, respectively. The time-averaged velocity profiles of blood flow were obtained with spatial resolutions of 8 × 0.8 μm and maximum velocity of 3 mm s^{-1}. These results were obtained by removing abnormal velocity vectors observed in instantaneous velocity distributions. These in vivo images were taken using an intravital microscope with a high-speed CCD camera, while illuminating with a 250 W direct-current metal halide lamp.

Bitsch et al. (2003, 2005) measured the velocity field of blood plug flow in a flat micro capillary in which a high intensity light-emitting diode (LED) was used for illumination. They prepared a suspension of red blood cells in an aqueous solution whose results were compared with those of a suspension of beads in water. The beads and RBCs were used as tracer particles for each experiment, and the volumetric flow rates for bead and RBC experiments were 50 nL s^{-1} and 167 nL s^{-1}, respectively. A cell-free boundary layer was estimated, and the effect of focal depth was discussed.

Lima et al. (2008a) proposed the RBC radial dispersion coefficient to quantitatively measure the radial motion of labeled RBCs in blood flow containing normal RBCs. Confocal micro-PTV was used to investigate the interaction of multiple labeled RBCs. They also investigated the effect of hematocrit (Hct 2–35%) and microvessel geometry on the properties of in vitro blood flow (Re = 0.003-0.005) in a glass capillary.

Lee and Kim (2005, 2006) developed X-ray μPIV to measure blood flow in an opaque microchannel such as a Teflon tube. RBCs were used as tracer particles, and their technique was verified to be valid as long as hematocrit is in the range of 20-80% (refer to Sect. 4.3 for an explanation of X-ray μPIV).

RBCs, however, must be carefully used as tracer particles. RBCs' velocity differs from plasma velocity since a thin layer near the vessel wall is depleted of RBCs due to the Fåhraeus-Lindquist effect (Vennemann et al. 2007). Therefore, instead of RBCs, platelets can be used as a tracer particles if accurate near-wall velocity measurements are required. Tangelder et al. (1986) have compared in vivo RBCs and platelets velocity profiles in arterioles of the rabbit mesentery using fluorescent-labeled RBCs and platelets. Sugii et al. (2005) have measured the maximum RBCs and plasma velocities (6.9 mm/s and 7.0 mm/s, respectively) in micro round tube in vitro using fluorescent-labeled RBCs and 1-μm fluorescent particles.

6.1.2 Addition of fluorescent particles as tracers

Instead of using only RBCs as tracer particles, fluorescent particles are used since RBCs do not perfectly follow the blood flow, even under steady low Reynolds number conditions (Poelma et al. 2008). Lima et al. (2006) developed a confocal μPIV system using spinning disks to measure velocity profile of in vitro blood flow (Re = 0.025) in a glass microchannel and achieved a spatial resolution of 28.24 μm × 18.83 μm. Fluorescent particles (representing a 0.1% by volume) were added into RBC suspension fluid which consisted of physiological saline with RBCs. This technique was extended to investigate the effect of RBCs on blood flow within a PDMS microchannel changing

haematocrit up to 17% at a normal Hct (20%) (Lima et al. 2007, 2008b).

6.1.3 *Embryonic heart flow field analysis*

Velocimetry techniques have also been used for in vivo flow field measurements in the embryonic heart of a zebrafish (Hove et al. 2003). Observing the pattern of blood flow in a developing heart gives insight into its role in cardiac morphogenesis. The zebrafish was chosen due to its small size, optical clarity, and external development. A variety of methods were employed in their in vivo analyses. First, high-speed confocal imaging of a fluorescent dye to label blood serum was used to visualize flow patterns inside the heart chambers. This technique enabled measurements of blood volume beating. In order to more precisely measure fluid velocity through the heart, PIV was used with small groups of erythrocytes as tracer particles. Hove et al. (2003) was able to measure intracardiac velocities around 0.5 cm s^{-1}, corresponding to enormous physiological high shear stresses (>75 dyne cm^{-2}), and visualize vortices inside the beating embryonic heart.

Chicken embryos have often been used to measure in vivo blood flow due to facile direct observation with a modified μPIV technique and, second, that their immune systems are in the early stages of development. Vennemann et al. (2005, 2006) measured velocity profiles of blood-plasma flow in the heart of a chicken embryo using fluorescent liposome spheres as tracer particles. Rhodamine was attached to liposome for imaging and then polyethylene glycol (PEG) was coated to prevent the protein deposition and reduce the interaction with the blood vessel wall. Highly unsteady blood flows in the developing ventricle and atrium of the embryo due to the beating heart was determined during the cardiac cycle (Fig. 11). Similar experiments on the blood flow in the chicken embryo were carried out by Lee et al. (2007) and Poelma et al. (2008). Polystyrene spheres coated with Rhodamine and PEG were injected into vitelline veins and the wall shear stress was calculated based on the measured velocity profile of the blood flow (Poelma et al. 2008, 2009). Alternatively, RBCs were used to measure velocity profiles of blood flow in extraembryonic venous and arterial blood vessels without the addition of any other tracer particles (Lee et al. 2007).

6.2 Velocity profile around adherent cell

The velocity profile around biological cells has been investigated with μPIV while the cells were attached to the wall of microchannel. Anderson et al. (2006) developed a computational model to calculate the velocity profiles and shear stress in three different types of commercially available cell flow/perfusion chambers, which was verified with experimental results. In addition, they used MLO–Y4 cells attached to the bottom layer of the channel to investigate the effect on flow properties.

Pommer and Meinhart (2005), on the other hand, investigated the velocity profiles around an adhered single red blood cell to estimate the distribution of fluid-induced shear stress (Fig. 12). Later, the technique was extended to obtain three-dimensional, three-component (3D–3C) velocity profiles using the estimated shear-stress distribution based on the 2D–2C velocity profiles at various locations in the out-of-plane direction. A single human red blood cell was adhered to the bottom plane of glass microchannel. The flow around the RBC was measured and the experimental results were compared with numerical simulations to estimate the uncertainty of both the in-plane and out-of-plane velocities. The spatial resolutions for the in-plane components and the out-of-plane direction were 3 μm and 2 μm, respectively. Then, 340-nm fluorescent polystyrene particles were added to a PBS/BSA solution which was pumped into the

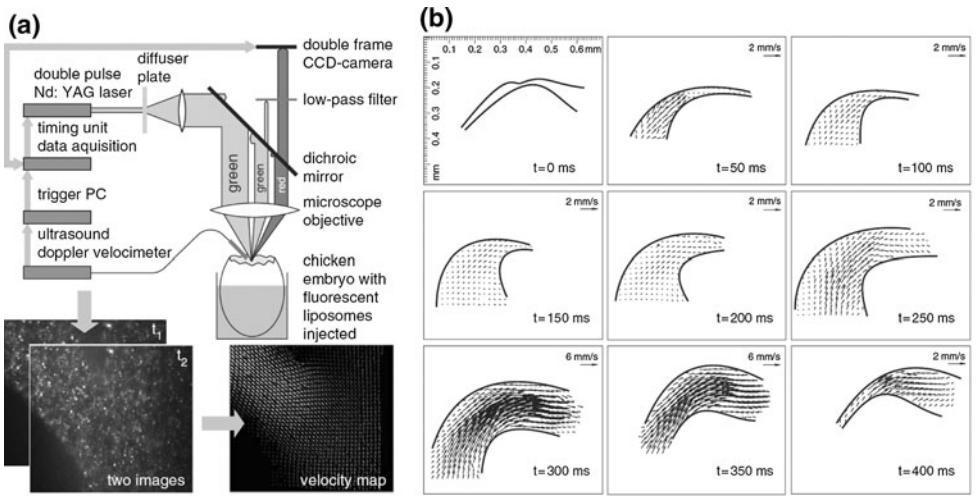

Fig. 11 In vivo μPIV of blood plasma in the heart of chicken embryo. **a** Schematic illustration of the experimental setup. **b** The velocity distributions in heart ventricle were obtained at nine consecutive points of the cardiac cycle when the ventricle is expanding and contracting. From Vennemann et al. (2006), with permission

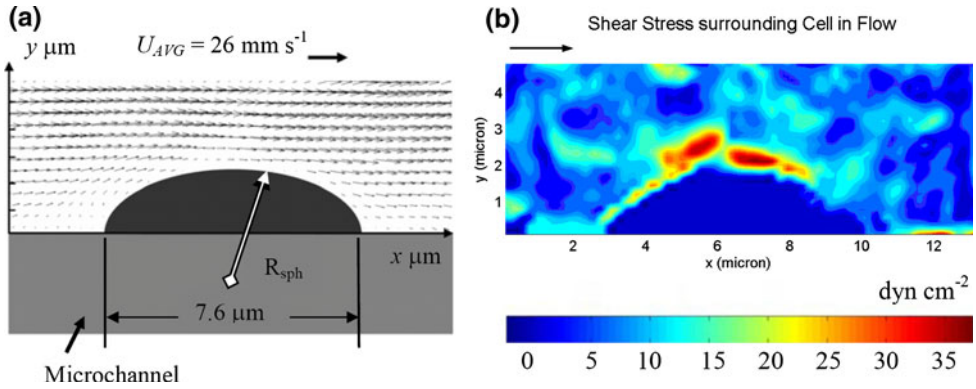

Fig. 12 μPIV measurement around an adherent red blood cell. **a** Velocity distribution; **b** shear stress. From Pommer and Meinhart (2005), with permission

microchannel (Pommer et al. 2007). Moreover, μPIV has been applied to investigate a monolayer of cells. Further, μPIV has been applied to investigate a monolayer of cells such as endothelial cells. The endothelial cells, which line the interior surface of blood vessels and are in direct contact with blood flow, are involved in the interaction between blood flow and the vessel wall such as the formation of new blood vessel (Poelma et al. 2009). Therefore, the wall shear stress acting on the endothelial cells is investigated by μPIV. The mean velocity distribution obtained from μPIV is widely used to calculate the wall shear-stress distribution with the assumption of Poiseuille flow with no-slip condition on the cultured endothelial cells (Rossi et al. 2006, 2008). Poelma et al. (2009), on the other hand, proposed two other methods to estimate the wall shear stress without the above flow assumption. The 3D distribution of wall shear stress was constructed in the outflow tract of an embryonic chicken heart using 1-μm fluorescent particles. Also, Long et al. (2004) measured blood viscosity and shear rate in a mouse cremaster-muscle venule by decreasing hematocrit, revealing that Poiseuille flow assumption with no-slip condition caused an underestimation of the shear rate.

6.3 Other biological analyses

Hirono et al. (2008) used μPIV methods to count biological cells flowing through a microchannel and measure their sizes. A technique called microfluidic image cytometry (μFIC) was proposed to investigate the detailed process of platelet aggregation; this technique was characterized choosing a 2-μm-diameter polystyrene particle, similar to the size of platelet. A sample of diluted, platelet rich plasma was used to validate μFIC, and its results were compared using a commercially available hemocytometry.

Petermeier et al. (2007) measured the fluid velocity profiles produced by the motion of microorganisms such as opercularia asymmetrica while using yeast cells as a tracer particle. Microorganismic flow generated from the movement of ciliates was analyzed using a neuronumerical hybrid method which detects artifacts in conventional PIV. This method can detect not only spurious velocity vectors but also additional phenomena like a moving boundary, which is present in investigated microorganisms.

Ichiyanagi et al. (2007) measured not only the velocity distribution with 1.0 μm tracer particles but also pH distribution using Fluorescein sodium salt, whose pH value is fluorescently dependent. Their investigation used a T-shaped microchannel, and their μPIV measurement technique had velocity and pH uncertainties of 5.5 μm/s and 0.23, respectively. This simultaneous measurement technique is valuable in investigating mixing processes and chemical reacting flow.

7 Conclusion

Since its introduction over a decade ago, there have been many advances and various applications of μPIV to examine and characterize microfluidic flows, as has been described earlier in this article. There is no doubt that this technique will continue to improve and evolve as novel imaging techniques develop, illumination sources become more reliable, and the performance and sensitivity of digital cameras improve. Technological advancements will continue to drive the trend to develop high resolution, 3D μPIV systems and techniques. Further, μPIV will become more prominent as and when these and other optical components realize cost reduction. μPIV has proven to be a valuable tool to characterize the behavior of microflows, and its recent advances have shown that it can be versatile and adaptable toward numerous investigations in nanotechnology and biotechnology. For example, recent extensions of X-Ray imaging and Nuclear Magnetic Resonance imaging (NMR or MRI) show the promise of imaging through channel walls and even fluids that are opaque at optical wavelengths. Despite these new modalities of imaging, the fundamental technique remains unchanged: correlation analysis combined with correlation averaging is used to track the motion of tracers. Ultimately, μPIV will be extended to many areas beyond its current scope of

applications and uses and become spatial and temporal resolutions driven to scales much lower than those existing in practice as of now.

References

Adrian RJ (1991) Particle-imaging techniques for experimental fluid mechanics. Annu Rev Fluid Mech 23:261–304

Adrian RJ (1996) Bibliography of particle image velocimetry using imaging methods: 1917–1995. University of Illinois at Urbana-Champaign, Urbana, IL

Adrian RJ (2005) 20 years of particle image velocimetry. Exp Fluids 39:159–169

Anderson EJ, Falls TD et al (2006) The imperative for controlled mechanical stresses in unraveling cellular mechanisms of mechanotransduction. Biomed Eng Online 5:27

Bitsch L, Olesen LH et al (2003) Micro PIV on blood flow in a microchannel. 7th international conference on miniaturized chemical and biochemical analysis systems. Squaw Valley, CA

Bitsch L, Olesen LH et al (2005) Micro particle-image velocimetry of bead suspensions and blood flows. Exp Fluids 39(3): 505–511

Born M, Wolf E (1999) Principles of optics: electromagnetic theory of propagation, interference and diffraction of light. Cambridge [England]; Cambridge University Press, New York

Bourdon CJ, Olsen MG et al (2004) Validation of analytical solution for depth of correlation in microscopic particle image velocimetry. Meas Sci Technol 15:318–327

Bourdon CJ, Olsen MG et al (2006) The depth of correlation in micro-PIV for high numerical aperture and immersion objectives. J Fluid Eng 128(4):883–886

Bown MR, MacInnes JM et al (2006) Three-dimensional, three-component velocity measurements using stereoscopic micro-PIV and PTV. Meas Sci Technol 17(8):2175–2185

Brown MR, Meinhart C (2006) AC electroosmotic flow in a DNA concentrator. Microfluid Nanofluid 2:513–523

Chamarthy P, Garimella SV et al (2009) Non-intrusive temperature measurement using microscale visualization techniques. Exp Fluids 47:159–170

Chuang HS, Wereley ST (2007) In vitro wall shear stress measurements for microfluid flows by using second-order SPE micro-PIV. Proceedings of IMECE2007, 2007 ASME international mechanical engineering congress and exposition. ASME, Seattle, WA, USA

Cowen EA, Monismith SG (1997) A hybrid digital particle tracking velocimetry technique. Exp Fluids 22:199–211

Csendes A, Szekely V et al (1996) Thermal mapping with liquid crystal method. Microelectron Eng 31:281–290

Curtin DM, Newport DT et al (2006) Utilising μ-PIV and pressure measurements to determine the viscosity of a DNA solution in a microchannel. Exp Thermal Fluid Sci 30:843–852

Dabiri D (2009) Digital particle image thermometry/velocimetry: a review. Exp Fluids 46:191–241

Devasenathipathy S, Santiago JG (2002) Particle tracking techniques for electrokinetic microchannel flows. Anal Chem 74:3704–3713

Devasenathipathy S, Santiago JG et al (2003) Particle imaging techniques for microfabricated fluidic systems. Exp Fluids 34(4):504–514

Dubsky S, Fouras A et al (2008) Three component, three dimensional X-ray particle image velocimetry using multiple projections. 14th international symposium on applications of laser techniques to fluid mechanics. Lisbon, Portugal

Freudenthal PE, Pommer M et al (2007) Quantum nanospheres for sub-micron particle image velocimetry. Exp Fluids 43(4): 525–533

Fujisawa N, Funatani S et al (2005) Scanning liquid-crystal thermometry and stereo velocimetry for simultaneous three-dimensional measurement of temperature and velocity field in a turbulent Rayleigh-Bernard convection. Exp Fluids 38(3):291–303

Gomez R, Bashir R et al (2001) Microfluidic biochip for impedance spectroscopy of biological species. Biomed Microdevices 3(3):201–209

Gorti VM, Shang H et al (2008) Immunoassays in nanoliter volume reactors using fluorescent particle diffusometry. Langmuir 24(6):2947–2952

Grier DG (2003) A revolution in optical manipulation. Nature 424(6950):810–816

Guasto JS, Breuer KS (2008) Simultaneous, ensemble-averaged measurement of near-wall temperature and velocity in steady micro-flows using single quantum dot tracking. Exp Fluids 45:157–166

Guasto JS, Huang P et al (2006) Statistical particle tracking velocimetry using molecular and quantum dot tracer particles. Exp Fluids 41:869–880

Gui L, Lindken R et al (1997a) Phase-separated PIV measurements of the flow around systems of bubbles rising in water. ASME-FEDSM97-3103, ASME. New York, USA

Gui L, Merzkirch W et al (1997b) Evaluation of low image density PIV recordings with the MQD method and application to the flow in a liquid bridge. J Flow Visual Image Process 4(4):333–343

Hagsater SM, Westergaard CH et al (2008) A compact viewing configuration for stereoscopic micro-PIV utilizing mm-sized mirrors. Exp Fluids 45:1015–1021

Han G, Breuer KS (2001) Infrared PIV for measurement of fluid and solid motion inside opaque silicon microdevices. Proceedings of 4th international symposium on particle image velocimetry. Gttingen, Germany

Hirono T, Arimoto H et al (2008) Microfluidic image cytometry for measuring number and sizes of biological cells flowing through a microchannel using the micro-PIV technique. Meas Sci Technol 19(2):025401-1–025401-13

Hoffmann M, Schluter M et al (2006) Experimental investigation of liquid-liquid mixing in T-shaped micro-mixers using μ-LIF and μ-PIV. Chem Eng Sci 61:2968–2976

Hohenegger C, Mucha PJ (2007) Statistical reconstruction of velocity profiles for nanoparticle image velocimetry. Siam J Appl Math 68(1):239–252

Hohreiter V, Wereley ST et al (2002) Cross-correlation analysis for temperature measurement. Meas Sci Technol 13(7):1072–1078

Hove JR, Koster RW et al (2003) Intracardiac fluid forces are an essential epigenetic factor for embryonic cardiogenesis. Nature 421(6919):172–177

Huang H, Dabiri D et al (1997) On errors of digital particle image velocimetry. Meas Sci Technol 8:1427–1440

Ichiyanagi M, Sato Y et al (2007) Optically sliced measurement of velocity and pH distribution in microchannel. Exp Fluids 43:425–435

Ichiyanagi M, Sasaki S et al (2009) Micro-PIV/LIF measurements on electrokinetically driven flow in surface modified microchannels. J Micromech Microeng 19:045021

Jin S, Huang P et al (2004) Near-surface velocimetry using evanescent wave illumination. Exp Fluids 37:825–833

Jones BJ, Lee P-S et al (2008) Infrared micro-particle image velocimetry measurements and predictions of flow distribution in a microchannel heat sink. Int J Heat Mass Transfer 51: 1877–1887

Joseph P, Tabeling P (2005) Direct measurement of the apparent slip length. Phys Rev E 71(3):035303

Kähler CJ, Scholz U et al (2006) Wall-shear-stress and near-wall turbulence measurements up to single pixel resolution by means of long-distance micro-PIV. Exp Fluids 41:327–341

Karri S, Charonko J et al (2009) Robust wall gradient estimation using radial basis functions and proper orthogonal decomposition (POD) for particle image velocimetry (PIV) measured fields. Meas Sci Technol 20:045401

Keane RD, Adrian RJ (1992) Theory of cross-correlation analysis of PIV images. Appl Sci Res 49(3):191–215

Kihm KD, Banerjee A et al (2004) Near-wall hindered Brownian diffusion of nanoparticles examined by three-dimensional ratiometric total internal reflection fluorescence microscopy (3-D R-TIRFM). Exp Fluids 37:811–824

Kim MJ, Breuer KS (2007) Use of bacterial carpets to enhance mixing in microfluidic systems. J Fluid Eng 129:319–324

Kim HJ, Kihm KD (2002) Two-color (Rh-B & Rh-110) laser induced fluorescence (LIF) thermometry with sub-millimeter measurement resolution. J Heat Transfer-Trans Asme 124(4):596–596

Kim GB, Lee SJ (2006) X-ray PIV measurements of blood flows without tracer particles. Exp Fluids 41:195–200

Kinoshita H, Kaneda S et al (2007) Three-dimensional measurement and visualization of internal flow of a moving droplet using confocal micro-PIV. Lab Chip 7:338–346

Klank H, Goranovic G et al (2002) PIV measurements in a microfluidic 3D-sheathing structure with three-dimensional flow behaviour. J Micromech Microeng 12(6):862–869

Kumar A, Williams SJ et al (2008) Experiments on opto-electrically generated microfluidic vortices. Microfluid Nanofluidics. doi: 10.1007/s10404-008-0339-8

Lee SJ, Kim GB (2003) X-ray particle image velocimetry for measuring quantitative flow information inside opaque objects. J Appl Phys 94(5):3620–3623

Lee SJ, Kim GB (2005) Synchrotron microimaging technique for measuring the velocity fields of real blood flows. J Appl Phys 97(6):064701

Lee SJ, Kim S (2008a) Micro holographic PTV measurements of Dean flows in a curved micro-tube. 14th international symposium of laser techniques to fluid mechanics. Lisbon, Portugal

Lee SJ, Kim Y (2008b) In vivo visualization of the water-refilling process in xylem vessels using X-ray micro-imaging. Ann Bot 101(4):595–602

Lee JY, Ji HS et al (2007) Micro-PIV measurements of blood flow in extraembryonic blood vessels of chicken embryos. Physiol Meas 28(10):1149–1162

Leonardo RD, Leach J et al (2006) Multipoint holographic optical velocimetry in microfluidic systems. Phys Rev Lett 96:134502

Li HF, Sadr R et al (2006) Multilayer nano-particle image velocimetry. Exp Fluids 41:185–194

Lima R, Wada S et al (2006) Confocal micro-PIV measurements of three-dimensional profiles of cell suspension flow in a square microchannel. Meas Sci Technol 17:797–808

Lima R, Wada S et al (2007) In vitro confocal micro-PIV measurements of blood flow in a square microchannel: the effect of the haematocrit on instantaneous velocity profiles. J Biomech 40(12):2752–2757

Lima R, Ishikawa T et al (2008a) Radial dispersion of red blood cells in blood flowing through glass capillaries: the role of hematocrit and geometry. J Biomech 41(10):2188–2196

Lima R, Wada S et al (2008b) In vitro blood flow in a rectangular PDMS microchannel: experimental observations using a confocal micro-PIV system. Biomed Microdevices 10(2):153–167

Lin D, Angarita-Jaimes NC et al (2008) Three-dimensional particle imaging by defocusing method with an annular aperture. Opt Lett 33:905–907

Lindken R, Westerweel J et al (2005) Development of a self-calibrating stereo-μ-PIV system and its application to the three-dimensional flow in a T-shaped mixer. 6th international symposium on particle image velocimetry. Pasadena, CA

Lindken R, Westerweel J et al (2006) Stereoscopic micro particle image velocimetry. Exp Fluids 41:161–171

Lindken R, Rossi M, et al (2009) Micro-particle image velocimetry (μPIV): recent developments, applications, and guidelines. Lab Chip

Liu D, Garimella SV et al (2005) Infrared micro-particle image velocimetry in silicon-based microdevices. Exp Fluids 38:385–392

Long DS, Smith ML et al (2004) Microviscometry reveals reduced blood viscosity and altered shear rate and shear stress profiles in microvessels after hemodilution. Proc Natl Acad Sci USA 101(27):10060–10065

Lu HW, Bottausci F et al (2008) PIV investigation of 3-dimensional flow in drops actuated by EWOD. 21st IEEE international conference on micro electro mechanical systems (MEMS 2008). Tucson, AZ

Malsch D, Kielpinski M et al (2008) μPIV-analysis of Taylor flow in micro channels. Chem Eng J 135S:S166–S172

Meinhart CD, Zhang HS (2000) The flow structure inside a microfabricated inkjet printhead. J Microelectromech Syst 9(1): 67–75

Meinhart CD, Wereley ST et al (1999) PIV measurements of a microchannel flow. Exp Fluids 27(5):414–419

Meinhart CD, Wereley ST et al (2000a) Volume illumination for two-dimensional particle image velocimetry. Meas Sci Technol 11(6):809–814

Meinhart CD, Wereley ST et al (2000b) A PIV algorithm for estimating time-averaged velocity fields. J Fluid Eng 122(2): 285–289

Meinhart C, Wang DZ et al (2003) Measurement of AC electrokinetic flows. Biomed Microdevices 5:139–145

Muwanga R, Hassan I (2006) Local heat transfer measurements on a curved microsurface using liquid crystal thermography. J Thermophys Heat Transfer 20:884–894

Natrajan VK, Christensen KT (2009) Two-color laser-induced fluorescent thermometry for microfluidic systems. Meas Sci Technol 20(1):015401

Neve N, Lingwood JK et al (2008) The μPIVOT: an integrated particle image velocimeter and optical tweezers instrument for microenvironment investigations. Meas Sci Technol 19(9): 095403

Olsen MG (2009) Directional dependence of depth of correlation due to in-plane fluid shear in microscopic particle image velocimetry. Meas Sci Technol 20(1):015402.1–015402.9

Olsen MG, Adrian RJ (2000a) Brownian motion and correlation in particle image velocimetry. Opt Laser Technol 32(7–8): 621–627

Olsen MG, Adrian RJ (2000b) Out-of-focus effects on particle image visibility and correlation in microscopic particle image velocimetry. Exp Fluids 29(7):S166–S174

Olsen MG, Bourdon CJ (2003) Out-of-plane motion effects in microscopic particle image velocimetry. J Fluids Eng-Trans Asme 125(5):895–901

Olsen MG, Bourdon CJ (2007) Random error due to Brownian motion in microscopic particle image velocimetry. Meas Sci Technol 18(7):1963–1972

Park JS, Kihm KD (2006a) Three-dimensional micro-PTV using deconvolution microscopy. Exp Fluids 40:491–499

Park JS, Kihm KD (2006b) Use of confocal laser scanning microscopy (CLSM) for depthwise resolved microscale-particle image velocimetry (mu-PIV). Opt Lasers Eng 44(3–4):208–223

Park CW, Kim GB et al (2004a) Micro-PIV measurements of blood flow in a microchannel. Conference on optical and diagnostics and sensing IV. San Jose, CA

Park JS, Choi CK et al (2004b) Optically sliced micro-PIV using confocal laser scanning microscopy (CLSM). Exp Fluids 37(1):105–119

Park JS, Choi CK et al (2005) Temperature measurement for a nanoparticle suspension by detecting the Brownian motion using optical serial sectioning microscopy (OSSM). Meas Sci Technol 16(7):1418–1429

Pereira F, Lu J et al (2007) Microscale 3D flow mapping with μDDPIV. Exp Fluids 42(4):589–599

Petermeier H, Kowalczyk W et al (2007) Detection of microorganismic flows by linear and nonlinear optical methods and automatic correction of erroneous images artefacts and moving boundaries in image generating methods by a neuronumerical hybrid implementing the Taylor's hypothesis as a priori knowledge. Exp Fluids 42(4):611–623

Peterson SD, Chuang HS et al (2008) Three-dimensional particle tracking using micro-particle image velocimetry hardware. Meas Sci Technol 19(11):115406.1–115406.8

Poelma C, Vennemann P et al (2008) In vivo blood flow and wall shear stress measurements in the vitelline network. Exp Fluids 45:703–713

Poelma C, Heiden KVd et al (2009) Measurements of the wall shear stress distribution in the outflow tract of an embryonic chicken heart. J R Soc Interface 7(42):91–103

Pommer MS, Meinhart CD (2005) Shear-stress distribution surrounding individual adherent red cells in a microchannel measured using Micro-PIV. 6th international symposium on particle image velocimetry. Pasadena, CA

Pommer MS, Kiehl AR et al (2007) A 3D-3C micro-PIV method. IEEE international conference of nano/micro engineered and molecular systems. Bangkok, Thailand

Pouya S, Koochesfahani M et al (2005) Single quantum dot (QD) imaging of fluid flow near surfaces. Exp Fluids 39(4):784–786

Prasad AK, Adrian RJ (1993) Stereoscopic particle image velocimetry applied to liquid flows. Exp Fluids 15:49–60

Raffel M, Gharib M et al (1995) Feasibility study of three-dimensional PIV by correlating images of particles within parallel light sheet planes. Exp Fluids 19:69–77

Raffel M, Willert CE et al (2007) Particle image velocimetry: a practical guide. Springer, Berlin, New York

Ravnic DJ, Zhang Y-Z et al (2006) Multi-image particle tracking velocimetry of the microcirculation using fluorescent nanoparticles. Microvasc Res 72:27–33

Robinson O, Rockwell D (1993) Construction of three-dimensional images of flow structure via particle tracking techniques. Exp Fluids 14:257–270

Ross D, Locascio LE (2003) Fluorescence thermometry in microfluidics. Temperature: its measurement and control in science and industry, vol 7

Ross D, Gaitan M et al (2001) Temperature measurement in microfluidic systems using a temperature-dependent fluorescent dye. Anal Chem 73(17):4117–4123

Rossi M, Ekeberg I et al (2006) In vitro study of shear stress over endothelial cells by Micro Particle Image Velocimetry (μPIV). 13th Int. Symp Appl. laser techniques to fluid mechanics. Lisbon, Portugal

Rossi M, Lindken R et al (2008) Single-cell level measurement of shape, shear stress distribution and gene expression of endothelial cells in microfluidic chips. 6th international conference on nanochannels, microchannels, and minichannels. Darmstadt, Germany

Sadr R, Yoda M et al (2004) An experimental study of electro-osmotic flow in rectangular microchannels. J Fluid Mech 506:357–367

Sadr R, Li HF et al (2005) Impact of hindered Brownian diffusion on the accuracy of particle-image velocimetry using evanescent-wave illumination. Exp Fluids 38(1):90–98

Sadr R, Yoda M et al (2006) Velocity measurements inside the diffuse electric double layer in electro-osmotic flow. Appl Phys Lett 89(4):044103

Sadr R, Hohenegger C et al (2007) Diffusion-induced bias in near-wall velocimetry. J Fluid Mech 577:443–456

Sakakibara J, Adrian RJ (1999) Whole field measurement of temperature in water using two-color laser induced fluorescence. Exp Fluids 26(1–2):7–15

Santiago JG, Wereley ST et al (1998) A particle image velocimetry system for microfluidics. Exp Fluids 25(4):316–319

Satake S, Kunugi T et al (2005) Three-dimensional flow tracking in a micro channel with high time resolution using micro digital-holographic particle-tracking velocimetry. Opt Rev 12(6):442–444

Satake S, Kunugi T et al (2006) Measurements of 3D flow in a micro-pipe via micro digital holographic particle tracking velocimetry. Meas Sci Technol 17:1647–1651

Sato Y, Irisawa G et al (2004) Visualization of convective mixing in microchannel by fluorescence imaging. Meas Sci Technol 14:114–121

Sheng J, Malkiel E et al (2006) Digital holographic microscope for measuring three-dimensional particle distributions and motions. Appl Opt 45(16):3893–3901

Shinohara K, Sugii Y et al (2004) High-speed micro-PIV measurements of transient flow in microfluidic devices. Meas Sci Technol 15:1965–1970

Shinohara K, Sugii Y et al (2005) Development of a three-dimensional scanning microparticle image velocimetry system using a piezo actuator. Rev Sci Instrum 76:106109

Sinton D (2004) Microscale flow visualization. Microfluid Nanofluid 1(1):2–21

Song H, Chen DL et al (2006) Reactions in droplets in microflulidic channels. Angew Chem Int Ed 45(44):7336–7356

Speidel M, Jonas A et al (2003) Three-dimensional tracking of fluorescent nanoparticles with subnanometer precision by use of off-focus imaging. Opt Lett 28(2):69–71

Squires TM, Quake SR (2005) Microfluidics: fluid physics at the nanoliter scale. Rev Mod Phys 77:977–1026

Sugii Y, Nishio S et al (2002) In vivo PIV measurement of red blood cell velocity field in microvessels considering mesentery motion. Physiol Meas 23(2):403–416

Sugii Y, Okuda R et al (2005) Velocity measurement of both red blood cells and plasma of in vitro blood flow using high-speed micro PIV technique. Meas Sci Technol 16(5):1126–1130

Tanaami T, Otsuki S et al (2002) High-speed 1-frame/ms scanning confocal microscope with a microlens and Nipkow disks. Appl Opt 41(22):4704–4708

Tangelder GJ, Slaaf DW et al (1986) Velocity profiles of blood-platelets and red-blood-cells flowing in arterioles of the rabbit mesentery. Circ Res 59(5):505–514

Tien W, Kartes P et al (2008) A color-coded backlighted defocusing digital particle image velocimetry system. Exp Fluids 44:1015–1026

Tretheway DC, Meinhart CD (2002) Apparent fluid slip at hydrophobic microchannel walls. Phys Fluids 14(3):L9–L12

Tretheway DC, Meinhart CD (2004) A generating mechanism for apparent fluid slip in hydrophobic microchannels. Phys Fluids 16(5):1509–1515

Vennemann P, Kiger K et al (2005) In vivo micro PIV in the embryonic avian heart. 6th international symposium on particle image velocimetry. Pasadena, CA, USA

Vennemann P, Kiger KT et al (2006) In vivo micro particle image velocimetry measurements of blood-plasma in the embryonic avian heart. J Biomech 39(7):1191–1200

Vennemann P, Lindken R et al (2007) In vivo whole-field blood velocity measurement techniques. Exp Fluids 42:495–511

Wang DZ, Sigurdson M et al (2005) Experimental analysis of particle and fluid motion in ac electrokinetics. Exp Fluids 38(1):1–10

Wang C, Nguyen NT et al (2007) Optical measurement of flow field and concentration field inside a moving nanoliter droplet. Sens Actuators A 133:317–322

Wereley ST, Gui L (2003) A correlation-based central difference image correction (CDIC) method and application in a four-roll mill flow PIV measurement. Exp Fluids 34:42–51

Wereley ST, Meinhart CD (2001) Adaptive second-order accurate particle image velocimetry. Exp Fluids 31(3):258–268

Wereley ST, Gui L et al (2002) Advanced algorithms for microscale particle image velocimetry. AIAA J 40(6):1047–1055

Wereley ST, Meinhart C et al (2005) Single pixel evaluation of microchannel flows. Proceedings of IMECE2005, 2007 ASME international mechanical engineering congress and exposition. Orlando, FL, USA, ASME

Westerweel J (1994) Efficient detection of spurious vectors in particle image velocimetry data. Exp Fluids 16:236–247

Westerweel J, Geelhoed PF et al (2004) Single-pixel resolution ensemble correlation for micro-PIV applications. Exp Fluids 37(3):375–384

Willert CE, Gharib M (1991) Digital particle image velocimetry. Exp Fluids 10:181–193

Willert CE, Gharib M (1992) 3-Dimensional particle imaging with a single camera. Exp Fluids 12(6):353–358

Wu MM, Roberts JW et al (2005) Three-dimensional fluorescent particle tracking at micron-scale using a single camera. Exp Fluids 38(4):461–465

Xia Y, Whitesides GM (1998) Soft lithography. Annu Rev Mat Sci 28:153–184

Yoon SY, Kim KC (2006) 3D particle position and 3D velocity field measurement in a microvolume via the defocusing concept. Meas Sci Technol 17(11):2897–2905

Zettner CM, Yoda M (2003) Particle velocity field measurements in a near-wall flow using evanescent wave illumination. Exp Fluids 34(1):115–121

Zhu LD, Tretheway D et al (2005) Simulation of fluid slip at 3D hydrophobic microchannel walls by the lattice Boltzmann method. J Comput Phys 202(1):181–195